(19) Di Nola, A.; Berendsen, H. J. C.; Hallenga, K., to be published.
(20) Liquori, A. M. *Q. Rev. Biophys.* **1969**, *2*, 65.
(21) IUPAC–IUB Commission on Biochemical Nomenclature *Biochemistry* **1970**, *9*, 3471.
(22) Hockney, R. W.; Eastwood, J. W. "Computer Simulations Using Particles"; McGraw-Hill, New York, 1981.
(23) Berendsen, H. J. C.; van Gunsteren, W. F.; Postma, J. P. M.; Haak, J. R.; Di Nola, A., *J. Chem. Phys.*, in press.
(24) Ryckaert, J. P.; Ciccotti, G.; Berendsen, H. J. C. *J. Comput. Phys.* **1977**, *23*, 327.
(25) Gō, N.; Scheraga, H. A. *Macromolecules* **1976**, *9*, 535.
(26) Fixman, M. *Proc. Natl. Acad. Sci. U.S.A.* **1974**, *71*, 3050.
(27) Berendsen, H. J. C.; van Gunsteren, W. F. In "Proceedings, NATO Advanced Study Institute on Physics of Superionic Conductors and Electrode Materials"; Perram, J. W., Ed.; Plenum Press: New York, 1983.
(28) van Gunsteren, W. F. *Mol. Phys.* **1980**, *40*, 1015.
(29) van Gunsteren, W. F.; Karplus, M. *Macromolecules* **1982**, *15*, 1528.
(30) Paterson, Y.; Némethy, G.; Scheraga, H. A. *J. Solution Chem.* **1982**, *11*, 831.
(31) Jaynes, E. T. *Phys. Rev.* **1957**, *106*, 620.

Why Does the Generalized Stokes–Einstein Equation Work?†

George D. J. Phillies

Department of Chemistry, The University of Michigan, Ann Arbor, Michigan 48109.
Received February 2, 1984

ABSTRACT: The generalized Stokes–Einstein equation (GSE) $D_m = D_s\beta(\partial\pi/\partial c)_{P,T}(1 - \phi)$ and various microscopic theories for the mutual diffusion coefficient D_m are compared with the available experimental data on solutions of rigid macromolecules. The GSE and microscopic theories do not agree; the bulk of the experimental data favors the GSE. Methods of modifying microscopic theories in order to obtain agreement with the GSE are considered. If one neglects the Oseen $(a/r)^1$ term in the cross-diffusion tensor, satisfactory results are obtained. A rationale for this neglect, based on the nonzero frequencies of molecular motions, is noted.

I. Introduction

Our objective in this paper is to compare the available experimental data on the diffusion of macroparticulate species at high concentration with some of the theories which have been proposed to explain this behavior. Two major classes of theory are noted: semimicroscopic theories and microscopic theories. In the microscopic theories, diffusion coefficients are calculated from ensemble averages over products of intermolecular potentials and hydrodynamic interaction tensors. In semimicroscopic theories, calculations are made in terms of concentration gradients, associated fluxes, and cross-diffusion tensors, but hydrodynamic and direct interactions between individual particles are not given a detailed representation. It is often not sufficiently emphasized that these two classes of theory do not make the same predictions for D at high concentration. Furthermore, within the class of microscopic theories, there are significant disagreements as to what quantities are to be averaged to obtain D.

Our major emphasis is on the behavior of rigid spheroidal macroparticles, primarily protein molecules and silica spheres. One could also consider the dynamics of interacting, flexible polymer chains. However, this latter problem is far more complex and has substantially more free parameters. It is here preferred not to treat the chain problem before the dynamics of points is demonstrably understood. The virtues of this choice are suggested in section IV.

Section II of this paper summarizes semimicroscopic and microscopic theories for D. Section III notes useful experimental data on this problem and makes a numerical comparison of various theories with experiment. In most cases, experiment is in good agreement with the semimicroscopic theory. A discussion is found in section IV.

II. Theories of the Diffusion Coefficients

As is well-known, a characterization of macroparticle diffusion requires two translational diffusion coefficients. One of these, the mutual diffusion coefficient D_m, describes the relaxation of a real concentration gradient by the Brownian motion of the individual macromolecules and by the intermacromolecular forces. The intermacromolecular forces are reflected in the excess chemical potential μ^e of the solute. The other diffusion coefficient, the self (or tracer) diffusion coefficient D_s, describes the motion of an individual solute molecule through a uniform solution. D_s may be obtained by labeling some of the solute molecules, establishing countervailing gradients in the concentrations of labeled and unlabeled molecules (so that the total solute concentration is everywhere the same), and measuring the relaxation of the labeled solute's concentration gradient.

Treatments based on irreversible thermodynamics, i.e., semimicroscopic treatments, obtain[1,2]

$$D_s = k_B T/f_s \tag{2.1a}$$

$$D_m = \left[\left(\frac{\partial\pi}{\partial c}\right)_{P,T}(1 - \phi)\right] \Big/ f_m \tag{2.1b}$$

Here, k_B is Boltzmann's constant, T is the absolute temperature, $(\partial\pi/\partial c)_{P,T}$ is the isothermal osmotic compressibility, f_s and f_m are the drag coefficients for self and mutual diffusion, $\beta = (k_B T)^{-1}$, and ϕ is the volume fraction of solute ($\phi = c\bar{v}$, $\bar{v}$ being the thermodynamic partial volume of the solute). From the Onsager reciprocal relations and the physical quasi-identity of labeled and unlabeled molecules, it is possible to construct a self-consistent treatment of D_s and D_m which relates f_s and f_m, indicating[3]

$$f_s = f_m \tag{2.2}$$

from which follows the generalized Stokes–Einstein equation[3] (GSE)

$$D_m = D_s\beta\left(\frac{\partial\pi}{\partial c}\right)_{P,T}(1 - \phi) \tag{2.3a}$$

or[4]

$$D_m = D_s[S(k)]^{-1}(1 - \phi) \tag{2.3b}$$

where $S(k)$ is the static structure factor at wave vector k.

†Support of this work by the National Science Foundation under Grant CHE82-13941 is gratefully acknowledged.

0024-9297/84/2217-2050$01.50/0

Equation (2.3b) applies to a sinusoidal concentration fluctuation of wave vector $|\mathbf{k}| = k$. The validity of eq 2.2 in very dilute solutions has not been questioned; however, in concentrated solutions the correctness of eq 2.2 is in dispute.

One may also attempt to calculate D_m on a microscopic level, taking into account direct and hydrodynamic interactions between the solute particles, rather than lumping all interactions into thermodynamic and frictional terms, as is done in the semimicroscopic theories. These microscopic theories do not yield the generalized Stokes–Einstein equations (2.3), because orthodox microscopic calculations indicate $f_s \neq f_m$. The direct forces most often included are the hard-sphere potential

$$U(r) = \infty, \quad r < 2a_I; \qquad U(r) = 0, \quad r > 2a_I \tag{2.4}$$

(where a_I is the range of the hard-core potential), the screened electrostatic potential

$$U(r) = \frac{Z^2e^2}{Ea(1 + \kappa a)^2}\,\frac{e^{-\kappa(r-2a)}}{r} \tag{2.5}$$

(where Ze and a are the macroparticle charge and radius, respectively, E is the solvent dielectric constant, and κ is the Debye screening factor), and the van der Waals potential.

Besides direct interactions, Brownian macroparticles are subject to the random solute–solvent forces which cause Brownian motion. The fluctuating hydrodynamic forces on a pair of particles are partially correlated, causing hydrodynamic interactions. The hydrodynamic interactions between a pair of spheres in solution are most often given in tensor form as[5,6]

$$\mathbf{b}_{ij}^{s} = -\frac{15}{4}\left(\frac{a}{r}\right)^4\hat{\mathbf{r}}\hat{\mathbf{r}} + \left(\frac{a}{r}\right)^6\left[\frac{105}{16}\hat{\mathbf{r}}\hat{\mathbf{r}} - \frac{17}{16}\mathbf{I}\right] \tag{2.6}$$

$$\mu_{ij} = \frac{1}{f_0}\left[\frac{3}{4}\frac{a}{r}(\mathbf{I} + \hat{\mathbf{r}}\hat{\mathbf{r}}) + \frac{1}{2}\left(\frac{a}{r}\right)^3(\mathbf{I} - 3\mathbf{rr}) + \frac{75}{4}\left(\frac{a}{r}\right)^7\mathbf{rr} + \ldots\right] \tag{2.7}$$

Here, $\mathbf{I}$ is the identity tensor, $\hat{\mathbf{r}}$ denotes the unit vector pointing from i to j, and η is the solvent viscosity. $\mathbf{b}_{ij}^{s}$ describes the retardation in the motion of i when a force is applied to i, due to the presence of a neighboring particle j. μ_{ij} characterizes the motion produced in a particle i when a force is applied to particle j, while $f_0 = 6\pi\eta r_0$.

The effects described in eq 2.4–2.7 are to be combined to determine D_s and D_m. For example, Beenacker and Mazur[7] give

$$D_s k^2 = \frac{1}{N}\sum_{i=1}^{n}\langle \mathbf{k}\cdot\mu_{ii}\cdot\mathbf{k}\rangle k_B T \tag{2.8a}$$

$$D_m k^2 = \frac{1}{N}\sum_{i,j=1}^{n}\langle \mathbf{k}\cdot(\mu_{ij} - \mathbf{S}_{ij})\cdot\mathbf{k}\rangle\,\frac{k_B T}{S(k)} \tag{2.8b}$$

where $\mathbf{S}_{ij}$ is a tensor, analogous to μ_{ij}, which gives the flow of fluid (rather than particles) induced at $\mathbf{r}_i$ ($\mathbf{S}_{ii} = 0$), $S(k)$ is the static structure factor at wave vector k (as in eq 2.3b), and the limit of small k has been taken.

$$\mu_{ii} = \frac{1}{f_0}[\mathbf{I} + \sum_{j\neq i}^{n}\mathbf{b}_{ij}^{s}] \tag{2.9}$$

On the other hand, this author has argued for the numerically similar form (ref 8, eq 4.6)

$$D_m k^2 = \frac{k_B T}{S(k)}\langle\sum_{i,j=1}^{n}\mathbf{k}\cdot(\mu_{ij} - \mathbf{S}_{ij} - \phi\mathbf{I})\cdot\mathbf{k}\rangle - \frac{k_B T}{S(k)}\langle\sum_{i,j=1}^{n}[e^{-i\mathbf{k}\cdot\mathbf{r}_{ij}} + 1]i\mathbf{k}\nabla{:}\mu_{ij}\rangle \tag{2.10}$$

Equations 2.8b and 2.10 agree if $\nabla\cdot\mu_{ij} = 0$, which is correct if one uses only low-order approximations (in a/r) for μ_{ij}. We will be concerned with more accurate forms for μ, for which $\nabla\cdot\mu$ effects, as represented explicitly in (2.10), cannot be neglected.

Equations 2.8–2.10 do not incorporate the effects arising from correlations between the direct forces and the fluctuating hydrodynamic forces. These effects manifest themselves as "dynamic friction", which changes the drag coefficients f_s and f_m. We have previously argued[9] that direct friction has equal effects on f_s and on f_m, at least to first order in the concentration. Experimental evidence that dynamic friction modifies f_s has recently been found.[10]

The semimicroscopic Stokes–Einstein equation predicts a specific relationship between four measurable quantities. On the other hand, the microscopic theories (eq 2.8–2.10) predict numerically the concentration dependence of D_s and D_m. A wide variety of calculations of D_s and D_m have appeared, differing in their approximations for the hydrodynamic interaction tensors, the potentials considered, and the order (in the concentration ϕ) to which they were carried out. If one expands D as

$$D_s = D_0(1 + k_s\phi + \mathcal{O}(\phi^2)\ldots) \tag{2.11a}$$

$$D_m = D_0(1 + k_m\phi + \mathcal{O}(\phi^2)\ldots)(1 - \phi) \tag{2.11b}$$

and treats a system with a hard-sphere potential, one finds from eq 2.8[5,7]

$$k_s = -1.735 \tag{2.12a}$$

$$k_m = +1.56 \tag{2.12b}$$

With the same hydrodynamic interaction tensor, eq 2.10 gives

$$k_m = -0.943 \tag{2.13}$$

Equation 2.12b neglects the modification of the $\nabla\cdot\mu$ terms. [The result $k_m = -3.625$ of ref 10 differs from eq 2.13 because $\mathbf{b}_{ij}^{s}$ and μ_{ij} were there treated to a significantly lower order in a/r.]

One may also consider more complex potentials. For example, one could assume that the hydrodynamic radius a and the hard-core radius a_I of eq 2.4 are not equal. This potential has been used as an approximation to the screened electrostatic potential. Noting that eq 2.8a and 2.10 take the forms

$$\phi k_s = 4\pi C_0\int r^2\,dr\,g(r)\left[-\frac{5}{4}\left(\frac{a}{r}\right)^4 + \frac{9}{8}\left(\frac{a}{r}\right)^6\right] \tag{2.14a}$$

$$\phi k_m = \phi k_s + 4\pi C_0\int r^2\,dr\left[g(r)\left(-\frac{5}{2}\left(\frac{a}{r}\right)^4 + \frac{301}{48}\left(\frac{a}{r}\right)^6 + \frac{450}{12}\left(\frac{a}{r}\right)^7\right)\right] - 4\pi C_0\int r^2\,dr\,(g(r) - 1)\left(\frac{a}{r}\right) \tag{2.14b}$$

where $g(r) = \exp(-\beta U)$ is the radial distribution function and $\hat{\mathbf{k}}$ is a unit vector, for $a_I \neq a$ one predicts

$$k_s = -\frac{15}{8}\frac{a}{a_I} + \frac{9}{64}\left(\frac{a}{a_I}\right)^3 \tag{2.15a}$$

$$k_m = -\frac{45}{8}\frac{a}{a_I} + \frac{355}{384}\left(\frac{a}{a_I}\right)^3 + \frac{450}{256}\left(\frac{a}{a_I}\right)^4 - 6\left(\frac{a_I}{a}\right)^2 \tag{2.15b}$$

Figure 1 plots k_s/k_s^0 and k_m/k_m^0 as functions of a_I/a, for $a_I > a$. Here, k_s^0 and k_m^0 are the values of k_s and k_m when $a_I = a$. $|k_s|$ is seen to fall by more than a factor of 2 at larger values of a_I. The behavior of k_s is readily

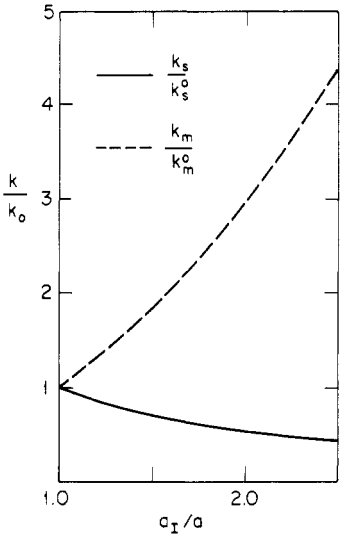

Figure 1. Concentration dependence of $D_s = D_0(1 + k_s\phi)$ and $D_m = D_0(1 + k_m\phi)[S(k)]^{-1}(1 - \phi)$ for hard spheres whose distances of closest approach $2a_I$ are larger than their hydrodynamic diameters $2a$. k_{s0} and k_m^0 are the values of k_s and k_m when $a_I = a$; see eq 2.14.

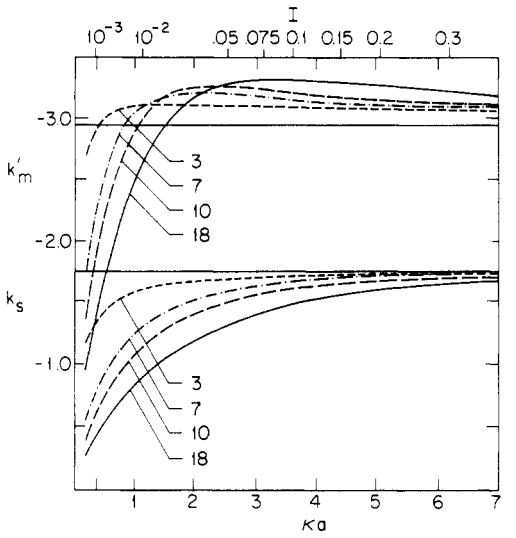

Figure 2. Values of k_s (eq 2.5) for hard spheres (a = 35 Å) with a screened electrostatic interaction as a function of the Debye screening length κ^{-1} and the corresponding ionic strength I of the solution for molecular charges Z = 3, 7, 10, and 18. Also shown is k_m', which is k_m calculated on the assumption that the $(a/r)^1$ term of eq 2.7 does not affect k_m, eq 2.14b. Other molecular parameters are given in the text.

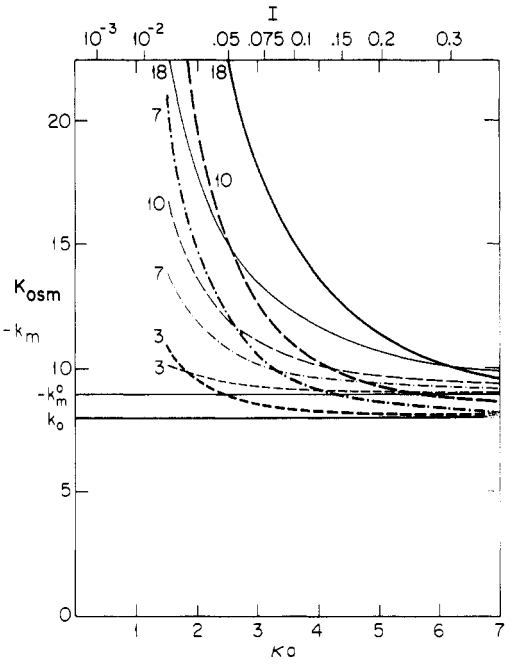

Figure 3. Values of k_m and k_{osm} (eq 2.11b or 2.14b and eq 2.17, respectively) for interacting hard spheres with a screened electrostatic potential, as shown in Figure 2.

understood: as a_I is increased, the likelihood of finding a pair of particles close to each other is reduced. This sort of increase in the average interparticle distance weakens the hydrodynamic interactions.

In contrast, as a_I/a is increased, $|k_m|$ increases sharply. This result conflicts with the usual intuition that hydrodynamic effects are weaker at large distances. The explanation is given by the physical nature of $\mu_{ij} - \mathbf{S}_{ij}$. If a force $\mathbf{F}_j$ is applied to particle j, that particle sets up a flow in the surrounding fluid. The flow, whose effects are described by $\mu_{ij} - \mathbf{S}_{ij}$, drags the other particles along with it. However, the fluid is incompressible; so the integrated flow across any surface which bisects the fluid volume must vanish. The flow parallel to $\mathbf{F}_j$ in the region near r_j is counterbalanced by a flow antiparallel to $\mathbf{F}_j$ in the region far from r_j. If particles are uniformly distributed in the fluid, then (ignoring gradient terms of higher order in a/r) the integrated particle flow $\int d\mathbf{s}\cdot\mathbf{J}_p$ will match the integrated fluid flow, so $\int d\mathbf{S}\cdot\mathbf{J}_p = 0$. The effect of interparticle interactions is to make the distribution of particles nonuniform, by moving particles between the regions within which $\mathbf{J}_s$ and $\mathbf{F}_j$ are parallel or antiparallel. In particular, a repulsive intermacromolecular interaction ($a_I > a$) expels particles from the region close to r_j within which $\mathbf{J}_s \| \mathbf{F}$; increasing a_I increases the number of expelled particles, thereby making the $\mu_{ij} - \mathbf{S}$ term more negative. As the range and strength of a repulsive solute–solute potential are increased, the Oseen hydrodynamic term $\int r^2\, dr\, (g(r) - 1)(a/r)$ becomes larger, making k_m more negative.

The relative values of k_s and k_m are as significant as their dependences on a_I/a. For simple hard spheres with $a_I = a$, the difference $|k_m - k_s|$ is 7.21. At larger a_I/a_H, $|k_m - k_s|$ becomes greater. This difference between k_m and k_s has serious implications for the generalized Stokes–Einstein equation. From the GSE (eq 2.3b and 2.11a) one has the semimicroscopic form

$$D_m = D_0(1 + k_s\phi)(1 - \phi)/S(k) \qquad (2.16a)$$

while the microscopic eq 2.8b and 2.11b give

$$D_m = D_0(1 + k_m\phi)(1 - \phi)/S(k) \qquad (2.16b)$$

For the hard-sphere potential, $k_m \neq k_s$. There are substantial numerical differences between these forms, so the microscopic theories based on eq 2.6–2.10 predict that the GSE (eq 2.16a) is not accurate.

To demonstrate that the result $k_m \neq k_s$ is not an artifact of a particular potential, numerical calculations of k_s and k_m were made by using eq 2.14 and the shielded electrostatic potential 2.5. Results of this calculation are found in Figures 2 and 3. It was assumed that a = 35 Å, $0.2 \leq \kappa a < 7$, $0 > Z > 18$, E = 81, and T = 298 K. These values are appropriate for bovine serum albumin (BSA) in the pH range 5.2–7.8. Within this range, BSA has a fixed conformation. For convenience, Figure 3 also shows k_{osm} where

$$S(k) = 1 + k_{osm}\phi = 1 + N\int r^2\, dr\, [g(r) - 1] \qquad (2.17)$$

It is not unknown to approximate hydrodynamic interactions with the Oseen tensor, for which

$$\mathbf{b}_{ij}^{s} = 0 \tag{2.18a}$$

$$\mu_{ij} = \frac{1}{f_0}\frac{3}{4}\frac{a}{r}[\mathbf{I} + \hat{\mathbf{r}}\hat{\mathbf{r}}] \tag{2.18b}$$

For this interaction, if one ignores dynamic friction one calculates $k_s = 0$ and

$$k_m = 4\pi C_0 \int r^2\, dr\, [g(r) - 1]\left(\frac{a}{r}\right) \tag{2.19}$$

For hard spheres with $a_I = a$, $k_m = -6$. It is not claimed that eq 2.19 should be even qualitatively correct, given the low caliber of the approximations (2.18) for μ. However, the Oseen approximation is often used in computations of polymer dynamics; the accuracy (or lack thereof) of eq 2.18 will be discussed below as casting light on the probable numerical accuracy of some theories of polymer motion. [Schurr[11] has argued that the $(1 - \phi)$ factor in D_m is extraneous, in that it is cancelled by a $(1 - \phi)^{-1}$ term in the proper definition of the thermodynamic force $(\partial\pi/\partial C_2)_{T,\mu_1}$.]

III. Experimental Findings

The experimental data needed for a comparison of the semimicroscopic and microscopic theories are available for three systems: hemoglobin in water, bovine serum albumin in water, and silica spheres in nonpolar solvents.

Jones et al.[12] obtained D_m for hemoglobin in 0.1 M KCl at the isoelectric pH over the concentration range 0–370 g·L^{-1}; a further study by Hall et al.[13] measured D_m for unliganded hemoglobin in 0.2 M phosphate buffer (pH 6.7) in the concentration range 8.6–157 g·L^{-1}. LaGatutta et al.[14] found D_m for hemoglobin in the pH range 6.3–7.7 for concentrations as high as 360 g·L^{-1} and at pH 6.7 for a range of ionic strengths. Of these results, the data of Hall et al. show the least random scatter. A thermodynamic factor equivalent to $(\partial\pi/\partial C)_{P,T}$ or $[S(k)]^{-1}$ for hemoglobin has recently been obtained from sedimentation and viscosity data by Minton and Ross.[15] Finally, Gros[16] obtained D_s for human and *Lumbricus terrestris* hemoglobin at pH 7.2–7.4 in 0.15 M NaCl for $20 \leq C \leq 433$ g·L^{-1}, while Keller et al. obtained D_s in 0.1 M phosphate buffer, pH 7.3, for $22 \leq C \leq 269$ g·L^{-1}.

Hall et al. and LaGattuta et al. present tests of eq 2.3, comparing their D_m data with the D_s values of Keller et al.[17] In both cases, eq 2.3 predicts the relative concentration dependences of D_s and D_m to within 10–15%, even though at large c, D_s and D_m differ by more than a factor of 2. If the D_s data of Gros are used, the agreement of D_s and D_m with eq 2.3 is substantially improved.

D_m of serum albumin has been obtained by Phillies et al.[18] in the pH range 4.5–7.6 for $5.0 < c < 340$ g·L^{-1} at a variety of ionic strengths. These data were compared with D_s values of Keller et al.[17] and osmotic pressure measurements by Scatchard and co-workers. While the D_m values are substantially less accurate than those of Hall et al., primarily because of advances in digital correlator technology over the past decade, the data of Phillies et al. did not disagree with eq 2.3, though D_m/D_s values as large as 3 were encountered. Root-mean-square fractional errors in tests of eq 2.3 with different albumin samples were ~12%. Probstein et al.[20] report indirect measurements of D_m for serum albumin under physiological conditions for c as high as 370 g·L^{-1}; these data are also in reasonable agreement with eq 2.3.

Kops-Werkhofen and co-workers have reported an elegant series of studies on synthetic silica spheres in various organic solvents.[21,22] By making a proper adjustment of the solvent composition and temperature, these spheres can be index matched by the solvent, allowing studies to be made on systems with concentrations as high as 0.86 g·cm^{-3} ($0 \leq \phi \lesssim 0.5$). D_m was obtained with quasi-elastic light scattering, while $S(k)$ was found from static light intensity measurements. D_s was obtained indirectly in two ways:

(i) For $c \gtrsim 0.4$ g·L^{-1}, the light scattering spectra showed two exponentials.[21] The theories of Weissman[23] and Pusey[24] for scattering by interacting polydisperse systems identify the faster exponential with D_m and the slower exponential with D_s.

(ii) By varying the synthetic pathway, it was possible to prepare silica spheres having different indices of refraction.[22] Index-matching techniques allow measurement of D of a dilute suspension of one type of sphere in a concentrated suspension of the other type of sphere. As the spheres were similar in size, this is a pseudo-tracer experiment which yields an approximate value for D_s.

Kops-Werkhofen and Fijnaut[21] compare D_s from method i with $D_m S(k)$ for silica spheres with $0.4 < c < 0.83$ g·L^{-1}. In this concentration range, D_m is virtually constant, while D_s/D_0 falls by a factor of nearly 20. Despite the huge change in D_s, $D_m S(k)$ and D_s agree with each other to within experimental error, as predicted by eq 2.3. This finding implies that $f_s = f_m$ at high concentrations. The assumption in ref 21 that at low concentration $f_s \neq f_m$ is a description of theoretical predictions and not a summary of experimental data.

On the other hand, by performing optical labeling of the silica spheres, Kops-Werkhofen et al.[22] found in our notation $k_s = -2.7 \pm 0.3$ and $k_m = 0.5 \pm 0.2$ at low concentration. Combinatin of their results for $[S(k)]^{-1}$ and D_s and eq 2.3b predicts, on the other hand, $k_m \cong 3.3 \pm 1.6$. The value for k_m obtained from the GSE is thus not consistent with this experiment. However, error bars on $S(k)$ were relatively large. Furthermore, D_s as obtained here was really a pseudo-tracer diffusion coefficient; the two sphere species are sufficiently mismatched that their sedimentation coefficients differ by 50%.

IV. Discussion

As seen in section III, the bulk of the available experimental data is consistent with the semimicroscopic eq 2.3. D_s, $(\partial\pi/\partial c)$ or $S(k)^{-1}$, D_m, and, by inference, the drag coefficients f_s and f_m all have strong concentration dependences. The available data do not prove that $f_s = f_m$. However, the success of the GSE, even when $S(k)^{-1}$ is as large as 3 or 20, indicates that effects which cause $f_s \neq f_m$ must be much weaker than effects which cause $S(k) \neq 1$. In terms of eq 2.11 and 2.16, most of the experimental data indicates that $|k_s - k_m| \ll |k_{osm}|$.

This inequality is not readily understood in terms of microscopic theories for the drag and diffusion coefficients. As seen in Figures 2 and 3, except for highly charged molecules at very low ionic strength, $-k_m$ and k_{osm} are roughly the same size. Both of these coefficients are much larger than k_s, so $|k_s - k_m|$ and $|k_{osm}|$ are nearly equal. Since k_m and k_{osm} tend to cancel, microscopic theories predict that D_m is nearly independent of solute concentration, as is indeed found in some (though not all) systems. However, the microscopic theories also state that $|k_s| \ll |k_m|$. If this inequality were true, $D_s\beta(\partial\pi/\partial c)(1 - \phi)$ would increase much more quickly than D_m, so that the difference between the GSE and the data for D_m would be comparable to the difference between the GSE and the data for D_s. The difference between the GSE and D_m is actually much less than the difference between the GSE and D_s.

One concludes that something appears to be significantly wrong, at least part of the time, with microscopic-hydrodynamic calculations of $\partial D_m/\partial c$ or $\partial D_s/\partial c$, in that exper-

iment supports the semimicroscopic generalized Stokes–Einstein equation, while the microscopic theories do not lead to this equation. Several possible explanations suggest themselves:

(1) The systems discussed in section III might all be sufficiently different from those on which microscopic calculations have been performed that the cited microscopic calculations are irrelevant, while correct microscopic calculations would give agreement with experiment. For the silica spheres, whose $S(k)$ obeys the expected hard-sphere equation, this explanation seems forced. For the protein molecules, one could invoke shape factors and change k_s or k_m, but at large $|Z|$ and small ka, shape effects should become less important.

(2) The standard microscopic calculations of D are all equivalent to the use of the generalized Smoluchowski equation

$$\frac{d}{dt}P(\mathbf{R}^n,t) = \sum_{i,j=1}^{n} \nabla_i \cdot \mathbf{D}_{ij} \cdot [\nabla_j P(\mathbf{R}^n,t) + \beta P(\mathbf{R}^n,t)\nabla_j U(\mathbf{R}^n,t)] \tag{4.1}$$

where $P(\mathbf{R}^n,t)$ is the probability density at $(\mathbf{R}^n,t)$, $U(\mathbf{R}^n,t)$ is the solute–solute potential, and $\mathbf{D}_{ij}$ is the diffusion tensor $\mathbf{D}_{ij} = \beta^{-1}\mu_{ij}$; $\mathbf{D}_{ii} = \beta^{-1}\mu_{ii}$. Historically, eq 4.1 was first proposed for noninteracting particles and then extended to treat sedimentation under the influence of an external potential. Use of eq 4.1 to calculate the behavior of interacting particles represents a further extension. The possibility that eq 4.1 must be modified to take into account correlations between Brownian motion and direct forces has been considered by several authors.[25-27] While there is substantial disagreement, our most recent calculations[9] indicate that D_s and D_m are modified to the same extent by these correlations, in which case these correlations are irrelevant to comparisons of the eq 2.3 and 2.8–2.10, at least to first order in ϕ.

(3) If $|k_{osm}| \approx |k_m|$, D_m is roughly independent of concentration, as seen in some data. If one also had $k_s \approx k_m$, as could happen if the equation for Ds contained a serious flaw, eq 2.3 would be preserved. One notes that in all three systems D_s changes more rapidly than called for by eq 2.15a. For example, Gros[16] finds $k_s = -6.7$ for hemoglobin.

(4) Finally, and most radically, the discrepancy could be due to the assumed integral form (2.14b) for k_m. The difference between k_s and k_m is primarily caused by the $(a/r)^1$ term of μ_{ij}. This result may be seen from Figure 2, which shows k_m', which is the value of k_m with the $\int r^2\,dr\,(g-1)(a/r)$ term deleted. As seen in Figure 2, $|k_m' - k_s| < 1.5$ for all values of Z and ka. As $k_{osm} \gg 1.5$, microscopic theories which replace k_m by k_m' will be in reasonable agreement with experiment.

What physical basis is there for eliminating the $(a/r)^1$ term of μ_{ij}? The Oseen tensor (2.18b) gives the response of the fluid to a steady force which has been applied for an infinite period of time. If one calculates the total momentum in the fluid flow responsible for the form of (2.18b), one obtains an integral which diverges as the volume of the container. In contrast, if two nearby particles are repelled from each other, the force between them lasts only a brief period of time and discharges a very small amount of momentum into the fluid. From momentum conservation, interacting particles therefore cannot create flows of the type of eq 2.18b. Similarly, the theory of fluctuating hydrodynamics predicts that Brownian motion is caused by stress fluctuations which create impulsive, not infinitely enduring, forces on the fluid.

While we observe diffusion over a long period of time, diffusive motion has a natural time scale $\mu_{ii} \cdot m$ determined by the mobility and mass m of the particle. The relaxation of even a macroscopic concentration gradient is due to many microscopic movements of the individual solute molecules and not to a steady zero-frequency drift of the solute. Diffusion is thus intrinsically a finite rather than a zero-frequency process.

The above doubts that μ are supported by recent work of van Saarloos and Mazur,[28] who calculated the hydrodynamic interactions between a pair of spheres undergoing nonsteady motion, concluding that the interaction is smaller than $(a/r)^1$ at short times, which is consistent with the difference between the impulsive forces which drive diffusion and the zero-frequency force which creates $(a/r)^1$ hydrodynamics. As long as consistent modifications are made in the cross-diffusion tensor $\mathbf{D}_{ij}$ and the mobility tensor μ_{ij}, the n-particle distribution functions will still be time-independent solutions to eq 4.1, as is required to obtain thermal equilibrium.

The use of frequency-dependent hydrodynamic interactions is not unknown in the literature. Burgers[29] reports a frequency-dependent equivalent of the Oseen tensor, in the form of a convolution integral. For a point source performing fixed-frequency harmonic oscillation, Chang and Mazo[30] obtain from the linearized Navier–Stokes equation and time-dependent viscosity a hydrodynamic interaction tensor which decays as R^{-3}, in accordance with the above. Ladanyi and Hynes[31] and McCammon and Wolynes[32] discuss how frequency-dependent hydrodynamics may affect chemical reaction rates, molecular vibrations, and vibrational line shapes in polymers and biopolymers.

Lastly, the rationale for ignoring work on polymer solutions is noted: Equations 2.18 and 2.19 yield simple microscopic forms for D_s and D_m. These forms are substantially inconsistent with experiment, both in that they predict D_s to be independent of ϕ and in that they predict $|k_s - k_m|$ to be large. As has been shown by Felderhof and others, using better values of μ gives more reasonable results for k_s. Many theories of polymer chain dynamics approximate the hydrodynamics with the simple Oseen tensor approximation (2.18). If it is at all correct, this approximation is entirely inadequate to treat solutions of spheres; at a minimum, one must incorporate corrections to $\mathbf{b}_{ij}^s$ and μ of higher order in a/r. A bead-and-spring model polymer differs from a sphere suspension in that the individual beads have a maximum as well as a minimum separation. The limit on the greatest possible distance between polymer beads will emphasize the importance of configurations with small a/r, so the high-order corrections to $\mathbf{b}_{ij}^s$ and μ should be *more* important in polymer solutions than in sphere suspensions. It follows that detailed numerical agreement between experiment and Kirkwood–Riseman (Oseen) type theories may well be fortuitous, though it is possible that the short-range hydrodynamic interactions primarily act by renormalizing the single-bead friction factor ζ.

In summary, a review of published experimental data[12-22] indicates that the generalized Stokes–Einstein equation (2.3) works much better than would be expected from detailed microscopic theories[5,6] for the diffusion coefficient. The relative success of the GSE in describing data, while not unknown, has been somewhat neglected; this paper seeks to redress this imbalance. A definitive explanation as to why the GSE works is *not* presented, but possible lines of attack for resolving the problem are suggested.

References and Notes

(1) C. Tanford, "Physical Chemistry of Macromolecules", Wiley, New York, 1965.

(2) M. M. Kops-Werkhofen and H. M. Fijnaut, *J. Chem. Phys.*, **77**, 2242 (1982).
(3) G. D. J. Phillies, *J. Chem. Phys.*, **60**, 983 (1974).
(4) B. J. Berne, in "Photon Correlation Spectroscopy and Velocimetry", H. Z. Cummins and E. R. Pike, Ed., Plenum Press, New York, 1977, p 344.
(5) B. U. Felderhof, *J. Phys. A*, **11**, 929 (1978).
(6) P. Mazur and W. van Saarlos, *Physica*, **115A**, 21 (1982).
(7) C. W. J. Beenacker and P. Mazur, *Phys. Lett. A*, **91**, 290 (1982).
(8) G. D. J. Phillies, *J. Chem. Phys.*, **77**, 2623 (1982).
(9) G. D. J. Phillies, *J. Chem. Phys.*, **74**, 260 (1981).
(10) G. D. J. Phillies, *J. Chem. Phys.*, **79**, 2325 (1983).
(11) J. M. Schurr, *Chem. Phys.*, **65**, 217 (1982).
(12) C. R. Jones, C. S. Johnson, Jr., and J. T. Penniston, *Biopolymers*, **17**, 1581 (1978).
(13) R. S. Hall, Y. S. Oh, and C. S. Johnson, Jr., *J. Phys. Chem.*, **84**, 756 (1980).
(14) K. J. LaGatutta, V. S. Sharma, D. F. Nicoli, and B. K. Kothari, *Biophys. J.*, **33**, 63 (1981).
(15) A. P. Minton and P. D. Ross, *J. Phys. Chem.*, **82**, 1934 (1978).
(16) G. Gros, *Biophys. J.*, **22**, 453 (1978).
(17) K. H. Keller, E. R. Canales, and S. I. Yum, *J. Phys. Chem.*, **75**, 379 (1971).
(18) G. D. J. Phillies, G. B. Benedek, and N. A. Mazer, *J. Chem. Phys.*, **65**, 1883 (1976).
(19) G. Scatchard, *J. Am. Chem. Soc.*, **68**, 2315 (1946); G. Scatchard, A. C. Batchelder, A. Brown, and M. Zoza, *J. Am. Chem. Soc.*, **68**, 2610 (1946); G. Scatchard, A. C. Batchelder, and A. Brown, *J. Am. Chem. Soc.*, **68**, 2320 (1946).
(20) R. F. Probstein, W. F. Leung, and Y. Alliance, *J. Phys. Chem.*, **83**, 1228 (1979).
(21) M. M. Kops-Werkhofen, H. J. Mos, P. N. Pusey, and H. M. Fijnaut, *Chem. Phys. Lett.*, **81**, 365 (1981).
(22) M. M. Kops-Werkhofen, C. Pathmamanoharan, A. Vrij, and H. M. Fijnaut, *J. Chem. Phys.*, **77**, 5913 (1982).
(23) M. B. Weissman, *J. Chem. Phys.*, **72**, 231 (1980).
(24) P. N. Pusey, *J. Phys. A*, **11**, 119 (1978).
(25) B. J. Ackerson, *J. Chem. Phys.*, **64**, 242 (1976).
(26) W. Dieterich and I. Peschel, *Physica*, **95A**, 208 (1979).
(27) S. Hanna, W. Hess, and R. Klein, *Physica*, **111A**, 181 (1982).
(28) M. van Saarloos and P. Mazur, *Physica*, **120A**, 77 (1983).
(29) J. M. Burgers, Second Report on Viscosity and Plasticity, Amsterdam Academy of Sciences, Amsterdam, The Netherlands, 1938.
(30) E. L. Chang and R. M. Mazo, *J. Chem. Phys.*, **64**, 1389 (1976).
(31) B. M. Ladanyi and J. T. Hynes, *J. Chem. Phys.*, **77**, 4739 (1982).
(32) J. A. McCammon and P. G. Wolynes, *J. Chem. Phys.*, **66**, 1452 (1977).

Radiation Cross-Linked Paraffins and Percolation Model

J. Stejny

H. H. Wills Physics Laboratory, University of Bristol, Bristol BS8 1TL, United Kingdom.
Received June 13, 1983

ABSTRACT: A percolation process on a lattice was used to model the cross-linking of paraffins induced by ^{60}Co γ-radiation. The molecular weight distribution of cross-linked paraffins was characterized by gel permeation chromatography (GPC). The GPC traces were compared with the chromatograms calculated from the size distribution of site clusters obtained by a random introduction of bonds into square, triangular, and Bethe lattices. The comparison revealed that the cross-linking produces significantly more of high molecular weight material and less of dimer than calculated from the models. This shows that the cross-linking is not random; the clustering of cross-links in paraffins is in excess of that predicted by percolation models based on random statistics. It was found that this excessive clustering is only little influenced by the state and crystallographic phase of the paraffins; hence more fundamental factors (recombination of radicals in spurs, chemical changes introduced by the cross-links) have to be responsible for this effect. However, it was confirmed that the crystal lattice has a profound influence on the position of the cross-links along the paraffin chains; in paraffin crystals the cross-links are more concentrated toward the chain ends than when irradiated in the melt. It was also confirmed that the crystallinity affects the cross-linking efficiency of the radiation; the yield of cross-linked material is higher if irradiated in the melt.

1. Introduction

Cross-linking and chain scission are the two major effects that determine the change of molecular weight in polymers subjected to ionizing radiation. In polyethylene and paraffin the cross-linking is dominant, resulting in a continuous increase of the molecular weight average with the dose and, finally, in the formation of an infinite network.[1,2] Because of its application the radiation-induced cross-linking of polyethylene was widely studied in the past[3] and it was found that most of the cross-links were located in the disordered, fold region of polyethylene crystals.[4-6] In contrast to polyethylene the crystallinity of paraffins is high and comparable with that of low molecular weight compounds. In paraffin crystals the chains are extended and the disordered regions associated with the chain folds in polyethylene are absent.[7] The molecular weight of paraffins is uniform and lower than in polyethylene, which simplifies the molecular weight analysis of the cross-linked products.

Two different techniques were used in the past for molecular weight analysis of cross-linked paraffins: gas chromatography (GLC)[8] and gel permeation chromatography (GPC).[9,10] The former technique is limited to low molecular weights only as the volatility of paraffins decreases rapidly with the molecular weight. This restriction does not apply to the GPC, which can be used in principle for all soluble polymers. However, in the molecular weight region common to both techniques, the resolution of GPC is inferior to GLC, which is capable of separating fully not only homologues of different molecular weights but also different isomers of the same molecular weight.[8]

In paraffin crystals the chains are fully extended and packed parallel in layers in a three-dimensional crystal lattice. If the linking of chain ends belonging to different layers is neglected, the intralayer cross-linking can be modeled by a percolation process on a two-dimensional lattice. The latter is constructed by the projection of chain axes onto a plane perpendicular to the chain direction.

In the percolation process[11] certain pairs of points (or sites) are connected and properties of such systems (size of clusters, their shape and density, appearance of an infinite size cluster, etc.) are studied.

0024-9297/84/2217-2055$01.50/0